Relevance of long-range screening in Mott transition examined via a hydrogen lattice

Zi-Jian Lang (郎子健),[1] Sudeshna Sen,[1,2] Pak Ki Henry Tsang,[3] Kristjan Haule,[4] Vladimir Dobrosavljević,[3,*] and Wei Ku (顧威)[1,5,6,†]

[1]*School of Physics and Astronomy, Shanghai Jiao Tong University, Shanghai 200240, China*
[2]*Department of Physics, Indian Institute of Technology (ISM) Dhanbad, Dhanbad 826004, India*
[3]*Department of Physics and National High Magnetic Field Laboratory, Florida State University, Tallahassee, Florida 32306, USA*
[4]*Center for Materials Theory, Department of Physics & Astronomy, Rutgers University, Piscataway, New Jersey O8854, USA*
[5]*Ministry of Education Key Laboratory of Artificial Structures and Quantum Control, Shanghai 200240, China*
[6]*Shanghai Branch, Hefei National Laboratory, Shanghai 201315, China*

(Received 29 August 2023; revised 20 April 2024; accepted 24 November 2025; published 22 December 2025)

The Mott transition, a metal-insulator transition due to strong electronic interaction, is observed in many materials without an accompanying change of system symmetry. An important open question in Mott's proposal is the role of long-range screening, whose drastic change across the quantum phase transition may self-consistently make the transition more abrupt, toward a first-order one. Here, we investigate this effect in a model system of hydrogen atoms in a cubic lattice, using charge self-consistent dynamical mean-field theory that incorporates approximately the long-range interaction within the density functional treatment. We found that the system is well within the charge-transfer (CT) regime and that the CT gap intimately related to the Mott transition closes smoothly instead. This indicates that the long-range screening does not play an essential role in this prototypical example. This finding can be understood from the fact that the obtained insulating phase in this model system is driven by strong local interaction, and the transition is associated with the closing of CT gap. Contrary to Mott's length-scale argument, such energetic competition between kinetic energy and local interaction is thus insensitive to long-range screening.

DOI: 10.1103/ydzp-l985

I. INTRODUCTION

Mott transition, as an interaction-driven metal-insulator transition (MIT) without the assistance of symmetry change, has continued to attract great attention in the past decades [1–3]. It describes the phase transition between a metal and a Mott insulator widely observed in strongly correlated materials, such as transition-metal oxides [4–8]. To date, Mott insulators have become one of the most important platforms for the exploration of strongly correlated physics such as unconventional superconductivity [4,9] and magnetism [10].

The unique characteristic of Mott insulators lies in their unexpected insulating behavior. Traditional insulators have their Bloch orbitals completely filled by electrons such that a finite energy scale is needed for the electrons to propagate without violating the Pauli principle. Mott insulators, on the other hand, do not satisfy this condition and therefore would appear metallic in standard band theories, indicating the need to include additional physics beyond the Pauli principle. To understand such insulating behavior, Mott [1,11] pointed out the importance of electronic interactions, under which the electrons in the system would reside in a bound state and thus be unable to propagate without overcoming the effective binding energy.

Following Mott's general picture, authors of modern theoretical studies [12,13] of Mott insulators typically use the half-filled Hubbard model [14–17] or its generalized form. For example, transition-metal oxides [4,6–8] and organic Mott insulators [18,19] have relatively strong local electronic repulsion U compared with the kinetic energy. In half-filled systems, such a large U pushes states with doubly occupied orbitals toward high energy and thus allows them to be integrated out from the low-energy sector, effectively leaving only singly occupied states without charge freedom (thus an insulator). From the perspective of Mott's picture, the repulsion U in such half-filled systems provides exactly the necessary electronic interaction to bind the electron in an effective local orbital.

Still, an important physics question remains open, namely, the role of the long-range Coulomb interaction on the nature of the quantum Mott transition. Mott argued [1,11] that, between the metallic and insulating phases, the significant change in the screening of long-range interaction could lead to a first-order MIT at zero temperature. In contrast, authors of current Hubbard model-based studies (which only incorporate local interaction) have found the quantum phase transition to be continuous [12,20] instead. It is therefore an important and timely task to investigate the role of long-range interaction on the Mott transition, particularly to examine the validity of Mott's expectation.

Here, to address this essential question, we attempt to incorporate the effect of long-range interaction and investigate the Mott transition of a model system with hydrogen atoms in a cubic lattice. The effect of interaction screening is incorporated approximately via density self-consistency [21,22] of the density functional theory plus dynamic mean-

*Contact author: vlad@magnet.fsu.edu.cn
†Contact author: weiku@sjtu.edu.cn

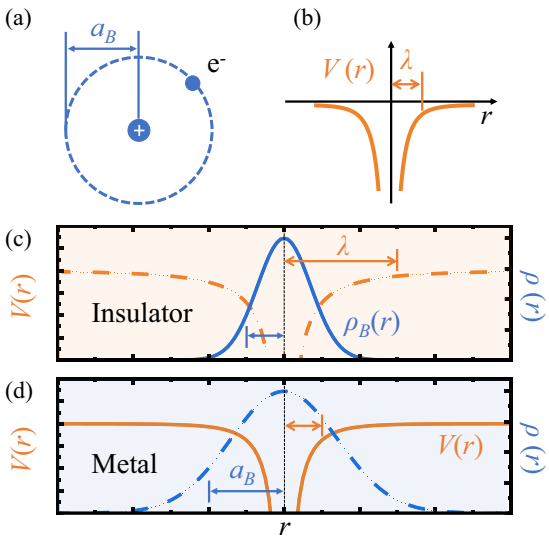

FIG. 1. Mott's picture of the key scales of MIT: (a) radius a_B of the particle-hole bound state, and (b) range λ of screened long-range Coulomb attraction $V(r)$ as a function of relative distance r. (c) When the bound state density ρ_B is confined within the Coulomb attraction $a_B < \lambda$, the system is insulating. (d) Otherwise, the system becomes metallic. The finite λ at the transition dictates a first-order phase transition in this picture.

field theory (DFT+DMFT; see Appendix for all calculation details) [12,13,23–29]. We found that this model system is in the charge-transfer (CT) regime, in which the relevant low-energy charge sector is dominated by the $2s$ and singly occupied $1s$ orbitals. Correspondingly, the Mott transition is intimately related to the closing of the CT gap. Importantly, the insulating gap is found to reduce smoothly to zero, and the charge carrier density (reflected by $1s$ orbital occupations) grows continuously. Both results suggest a continuous quantum phase transition, instead of the first-order transition expected by Mott's consideration of long-range screening. Our result can be understood from the fact that this common type of Mott transition in materials is mainly controlled by competition between kinetic and local interaction energies. Contrary to Mott's length-scale argument, such an energetic competition is therefore insensitive to screening of long-range interaction.

II. MOTT'S PICTURE

Let us first review the original consideration of the Mott transition. Mott proposed that a lattice of one-electron atoms, such as hydrogen, must be an insulator at large lattice spacing. This is because, starting from a ground state with a uniform charge of one electron per atom, the low-energy current response must be gapped associated with the formation of particle-hole bound states with an effective Bohr radius a_B [cf. Fig. 1(a)] (assuming a poorly screened e^2/r attractive Coulomb interaction over distance r.) On the other hand, at small lattice spacing, the system is expected to become a good metal with the lowest energy band half-filled. This is because the current response now turns gapless in association with the delocalization of particle-hole pairs, as a result of the long-range screening that reduces the range of the attraction $-(e^2/r)\exp(-2\pi r/\lambda)$ to a finite length scale λ [cf. Fig. 1(b)]. Therefore, in such a length-scale consideration, there must exist a transition point for a MIT at some intermediate lattice spacing.

As a simple estimation, Mott proposed that the MIT would take place at the point when a_B and λ are equal. This seems quite reasonable since, at $a_B \ll \lambda$ [cf. Fig. 1(c)], the bound state is well preserved such that the system should be a good insulator, while at $a_B \gg \lambda$ [cf. Fig. 1(d)], the interaction is screened too strongly to maintain a bound state such that the system would be a good metal. Based on this rough criteria, Mott estimated the critical density $n_c^{1/3} a_B \sim 0.25$ [30] via Thomas-Fermi approximation. Though this estimation is very crude, the criteria works very well for many materials [2].

The necessity of a finite $\lambda \sim a_B$ in Mott's criterion of MIT strongly suggests that the transition be first-order since a finite λ corresponds to a finite itinerant carrier density. As another way to visualize this, near the critical density, a slight increase of itinerant electrons would lead to an enhanced screening (or reduced λ), which in turn further increases the carrier density. One would therefore expect that such nonlinear feedback can lead to a discontinuous transition at zero temperature. Unfortunately, due to the complexity of quantum many-body problems, authors of theoretical studies to date have not been able to incorporate the screening of the length scale of long-range interactions, nor has the corresponding first-order quantum phase transition been obtained [12,13].

III. METHOD

To include this important screening effect of long-range Coulomb interaction beyond the Thomas-Fermi approximation, we use the density self-consistency scheme [21,22] of DFT+DMFT [7,31–35], with previously established double counting formulation [22]. In the process of self-consistent iteration, the change of electron density and the corresponding screening effect will feedback to the next iteration and thus allow the possibility of the first-order transition. The strong intra-atomic repulsion U ($\sim$1 Ry [36]) is included via DMFT [12,13,25–29], which is so far the most widely applied approximation to achieve the Mott insulating phase. This scheme is implemented by the DFT+ embedded DMFT (eDMFT) functional [21,22].

IV. RESULTS

We first start with a low-density insulating case at lattice spacing $a = 3.0$ Å. Figure 2(a) shows the resulting density of states (DOS) in the standard DFT calculation via local density approximation (LDA) [23,24]. As expected, the system is incorrectly identified as a metal with the chemical potential in the middle of the first band, corresponding to the half-filling $1s$ orbital. Upon inclusion of strong local exchange-correlation via DMFT at $T = 0.01$ eV, Fig. 2(b) shows the correct insulating state with a DOS hosting a gap around the chemical potential.

It is obvious that this insulating gap is not the standard Mott gap in a Hubbard model since its size (see Appendix A for

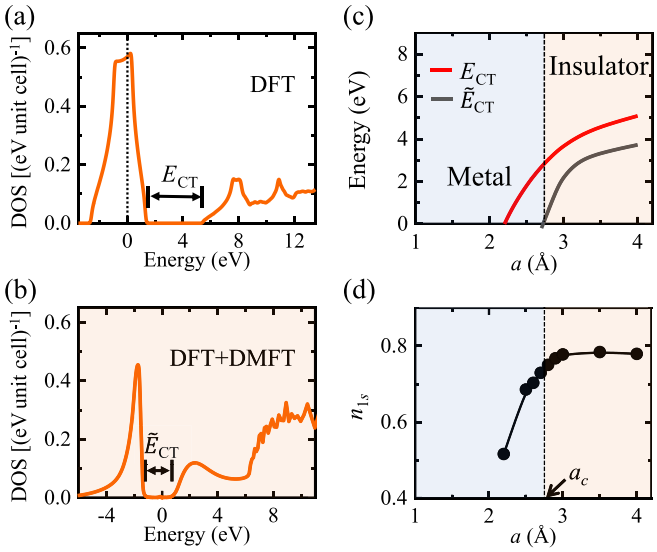

FIG. 2. (a) One-body DOS in units of $(\text{eV unit cell})^{-1}$ for $a = 3.0$ Å via standard DFT treatment, indicating a metallic system with a CT gap E_{CT} above the chemical potential set as the reference energy at zero. (b) The same via DFT+DMFT at $T = 0.01$ eV, giving an insulating system with a correlation-renormalized CT gap $\tilde{E}_{CT}$ across the chemical potential. (c) Smooth reduction of CT gap E_{CT} and $\tilde{E}_{CT}$ as the lattice constant a decreases toward the quantum critical point at a_c, below which $\tilde{E}_{CT} < 0$, and the system turns metallic with a gradual increase of itinerant hole carrier density reflected by the smooth reduction of $1s$ occupation within a fixed atomic sphere (d). Both (c) and (d) indicate a continuous quantum phase transition different from Mott's proposal.

the determination of CT gap E_{CT} and renormalized CT gap $\tilde{E}_{CT}$) [38] is only around 2 eV in this case, much smaller than the local repulsion $U \sim 1$ Ry. Indeed, in both DFT [panel (a)] and DFT+DMFT [panel (b)] results, the orbital content right above the gap is predominately of $2s$ and $2p$ instead of $1s$. Therefore, within the parameter range near the Mott transition, this model system is well within the CT insulator regime, in which the lowest-energy charge fluctuation is between $1s$ and $2s/2p$ orbitals of neighboring atoms.

Notice that the CT gap E_{CT} is strongly reduced from 4 eV in the DFT result [panel (a)] to only ∼2 eV in the DFT+DMFT result [panel (b)]. This can be understood from the additional energy lowering from the emergent antiferromagnetic spin exchange between the itinerant carrier in $2s/2p$ and the local immobile $1s$ spin, similar to the one that drives the formation of Kondo singlet [37,38].

Now approaching the metal-insulating transition via reducing the lattice constant, as shown by the black line in Fig. 2(c), the CT gap of the insulating solution reduces and eventually vanishes around $a = a_c \sim 2.8$ Å. Naturally, after that, the insulator solution can no longer be found and the system is metallic. Incidentally, for $a > a_c$, the metallic solution is unstable as well. This indicates that the phase transition is intimately related to the gap closing. (Note that, in an extremely narrow range of $\Delta a \sim 0.003$ Å around a_c, both metallic and insulating solutions can be found (cf. Appendix B). Considerations on this nearly negligible and somewhat artificial feature will be discussed later.)

Most importantly, our results display a very important deviation from Mott's expectation on the phase transition. Figure 2(c) shows that, even with the long-range Coulomb interaction and its screening incorporated via the DFT treatment, as the lattice spacing decreases, $\tilde{E}_{CT}$ only smoothly reduces to zero. Furthermore, as the lattice spacing decreases further, Fig. 2(d) shows that the occupation of the $1s$ orbital (within a fixed atomic sphere [39] of radius 1.8 a.u.) decreases smoothly as well, indicating a gradual development of hole carrier density. No abrupt enhancement of gap closing or the hole carrier density is found at a_c that corroborates Mott's expectation of a first-order phase transition. Clearly, our results suggest a continuous MIT. In other words, within the approximation of the state-of-the-art DFT+DMFT approach (omission of nonlocal correlation), the proposed drastic effect of screening of long-range interaction does not appear to be essential to the Mott transition in this model system.

V. DISCUSSION

This lack of relevance of long-range screening can be understood from the following energetic considerations of this model system. In this charge transfer insulator, mobile carriers can only occur in the ground state when the fully renormalized bandwidths grow to overcome the orbital energy and eliminate the indirect normalized CT gap minimum $\tilde{E}_{CT}$ [between momentum (π, π, π) and $(\pi, 0, 0)$]. However, this system has a rather large orbital energy difference (∼10 eV) between the dressed $2s$ and $1s$ orbitals and a large kinetic energy represented by the bandwidths of the dressed $1s$ band ($W_{1s} \sim 5$ eV) and the dressed $2s$ band ($W_{2s} \sim 20$ eV). Both of these key high-energy factors are insensitive to long-range interaction and thus its screening. Particularly, no dramatic change of long-range screening (of wave vector $q \sim 0$) is expected even right before the indirect gap is closed since the direct gap remains very large, of 10 eV scale.

In real materials, even beyond this point of gap closing, the mobile electrons in the dressed $2s$ orbital and holes in the dressed $1s$ orbital may still be bound into charge-neutral excitons by the long-range interactions. To such an excitonic insulator [40,41], Mott's consideration of the insulating phase in Fig. 1(c) may apply, in which the length scale of the long-range interaction is longer than the size of the bound excitons. Nevertheless, given that such excitonic binding should be of the order of 100 meV at best, two orders of magnitude weaker than the above kinetic energies, such an excitonic insulating phase, if present, must only delay the emergence of metallic carriers in a negligibly narrow region. Consequently, only a small number of carriers would be present when entering the metallic phase. Furthermore, this excitonic effect would be greatly suppressed by the dramatic difference in the effective masses of the electrons and holes. Therefore, even if Mott's proposal of a first-order transition may be realized here, the effect is likely too weak for the accuracy of realistic many-body calculations to date. On the technical side, such excitonic physics that involves nonlocal particle-hole pairs is surely beyond the capability of the LDA+DMFT framework employed in this study or even the advocated GW+eDMFT framework [42–45].

Our conclusion and the analysis above are qualitatively different from those of the previous extended DMFT studies on the extended Hubbard model [42–53], in which authors found a first-order quantum phase transition instead [46]. Note that those results originate from the nonlinear feedback in mapping the long-range Coulomb interaction onto retarded (dynamical) screening of local U of the Kondo impurity model. Such a mechanism is therefore physically distinct from (and unable to address) Mott's proposal of screening the length scale of long-range interaction. In contrast, the key factor for the MIT here is the closing of the indirect charge transfer gap, which is insensitive to the long-range screening. Correspondingly, a smooth continuous transition naturally results in our case.

Finally, it is well known [12,13,54] that the lack of interatomic correlation in DMFT treatments can lead to an unphysically large degree of degeneracy and, in turn, an artificially large entropy at finite temperature $T = 0^+$. This often causes an entropy-driven first-order transition at finite temperature [55,56]. Our finite-temperature calculation and the effective analytical model above are not immune to this problem (cf. Appendix B). Nonetheless, it is interesting to note that this artifact is much weaker in this model CT system than that in the Hubbard model. In fact, in Fig. 2(c), the region hosting first-order transition is narrower than the thickness of the black line. We take it that this distinction reflects the more robust continuous nature of the quantum phase transition in such CT systems.

Experimentally, our model system of a periodic hydrogen lattice could be tested by the next generation of capabilities that engineers a hydrogenlike lattice of any desired geometry through scanning tunneling microscopy—implanting donors on surfaces of semiconductors [57]. These experimental advances allow tuning the system across Mott transition without randomness and are thus ideal to experimentally clarify the role of long-range interaction.

VI. CONCLUSION

In summary, we investigate the important open question concerning the role of long-range screening on the quantum Mott transition using a model system of hydrogen lattice. We employ the charge self-consistent scheme of the DMFT that incorporates approximately the long-range interaction and its screening within the density functional treatment. The system is found to be well within the CT regime, and the CT gap closes smoothly across the quantum phase transition. Together with a gradually increasing hole carrier density in the metallic phase, this indicates a continuous quantum phase transition distinct from Mott's proposal. This deviation from Mott's long-range screening-based first-order picture can be understood from the following: (1) The obtained insulating phase in this typical case is driven by short-range interaction, and (2) the MIT involves the closing of the screening-insensitive CT energy, instead of length-scale switching proposed by Mott. Quantum MITs in such CT materials are thus insensitive to the long-range interaction. In this study, we leave open the finite possibility of a weak excitonic insulating phase in a very narrow region, in which Mott's picture might still apply. Further resolution of this possibility would require a significant advance in current computational capability.

ACKNOWLEDGMENTS

We thank Yuting Tan and Xinyi Li for their helpful discussions. This work is supported by National Natural Science Foundation of China under Grants No. 12274287 and No. 12042507, and Innovation Program for Quantum Science and Technology Grant No. 2021ZD0301900. S.S. acknowledges support from the Science and Engineering Research Board, India (Grants No. SRG/2022/000495 and No. MTR/2022/000638), and IIT(ISM) Dhanbad [Grant No. FRS(175)/2022- 2023/PHYSICS]. Work in Florida (V.D. and P.K.H.T.) was supported by National Science Foundation (NSF) Grant No. DMR-2409911, and the National High Magnetic Field Laboratory through NSF Cooperative Agreement No. DMR-2128556 and the State of Florida. K.H. was supported by NSF DMR-2233892.

APPENDIX A: CALCULATION DETAILS

Our self-consistent DFT+DMFT calculation employs an implementation [21,22] of the eDMFT method [12,13] based on the WIEN2K package [39]. The double-counting choice is exact [22]. We set a model system with a simple cubic hydrogen lattice with various lattice constants and a fixed on-site interaction $U = 1$ Ry on the $1s$ orbital. With the decrease of lattice constant, the kinetic hopping between atoms increases. A large energy window $[-30$ eV, 30 eV$]$ is used in defining the quantum Hilbert space that provides channels for various hopping and CT processes. The real-frequency dependence of the DOS is obtained from analytical continuation via the maximum entropy method [58] from the Matsubara-frequency Green's function.

The bare CT gap E_{CT} is determined from the DOS of the DFT calculation where the value of DOS goes to zero. This however is not applicable in the DFT+DMFT calculations in which the DOSs are obtained by the maximum entropy method [58] such that the DOS can never reduce to absolute zero. The CT gap (insulating gap) $\tilde{E}_{\mathrm{CT}}$ in the DFT+DMFT calculation shown in Fig. 1(c) is determined by the linear extrapolation near the gap edge, as shown in Fig. 3(a). Since the gaps are estimated in the regime far away from the phase

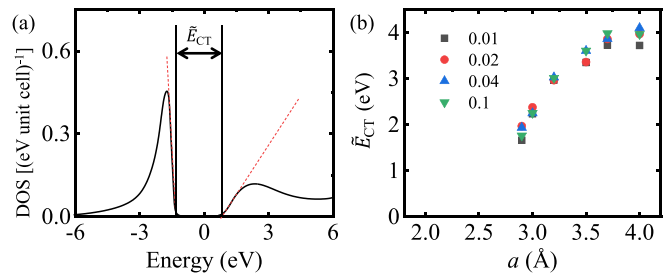

FIG. 3. (a) Determination of the CT gap (insulating gap) $\tilde{E}_{\mathrm{CT}}$ in the DFT+DMFT calculation. Red dashed line is the linear extrapolation near the edge of the gap. (b) CT gap $\tilde{E}_{\mathrm{CT}}$ as a function of lattice spacing a at temperature 0.1 eV (green triangle), 0.02 eV (blue triangle), 0.04 eV (red circle), and 0.01 eV (black square).

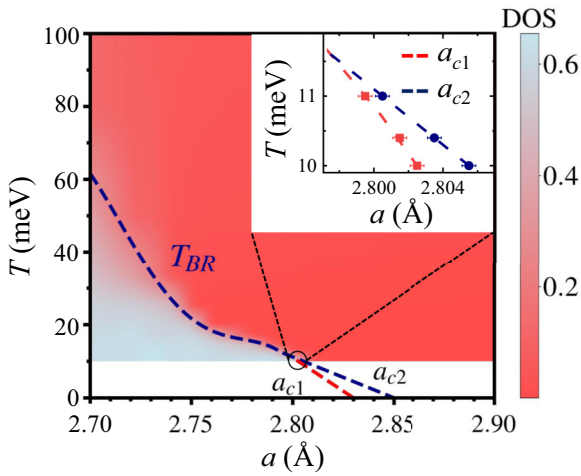

FIG. 4. Phase diagram of a real hydrogen lattice as a function of temperature and the lattice constant. The color map shows the value of the DOS at the chemical potential. Two dashed lines are the boundary of the coexistent region. The dark blue line $T_{\mathrm{BR}}(a)$ is the Brinkman-Rice line marking the thermal destruction of metallic quasiparticles [59]. The inserted figure is the coexistent region with two boundaries $a_{c1}(T)$ and $a_{c2}(T)$ denoted by red and dark blue dashed lines, respectively.

transition, they are barely influenced by the temperature, which is much smaller than these gaps in the energy scale, as shown in Fig. 3(b). One can find that the gaps remain almost the same upon increasing the temperature from 0.01 to 0.1 eV.

APPENDIX B: ENTROPY-DRIVEN FIRST-ORDER PHASE TRANSITION

It is well known that DMFT calculation at finite temperature suffers from the lack of nonlocal correlation, which introduces a large entropy contribution of the local spin even at $T = 0^+$ [54]. For the particular issue of Mott transition, such a large entropy is known to lead to a first-order phase transition at finite temperature calculation [12,13], even though the quantum phase transition is continuous. For the typical one-band case, there is a coexistent region which suggests a first-order phase transition. In our model system, if one carefully tunes the lattice space, the coexistent region can be still found in an extremely tiny region. As shown the inserted figure in Fig. 4, we also find a coexistent region below $T \sim 10$ meV with an extremely narrow size which demonstrates a first-order phase transition at finite temperature. This phase transition is, however, driven by the entropy instead of the screening effect suggested by Mott. More importantly, this artificially large entropy does not affect the continuous nature of the quantum phase transition.

It is interesting to note that, compared with the coexistent region of the typical one, there are two main differences. First, the value of critical on-site repulsion U_c is much larger. Usually, $U_c \sim 2\mathrm{D}$ is approximately equal to the bandwidth, while here, $U_c \sim 5\mathrm{D}$ is in great contrast with the single-band Hubbard model (D is half of the bandwidth in the LDA calculation, which is about 2 eV near $a \sim 2.8$ Å). This is not surprising because the transition is controlled by the energy

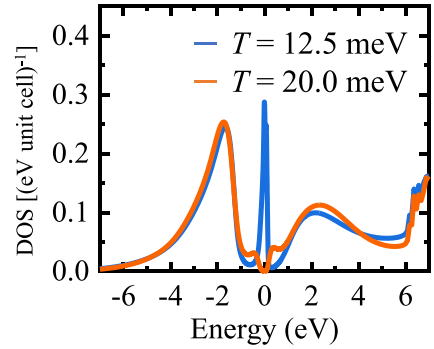

FIG. 5. DOS corresponds to $a = 2.78$ Å, on the metallic side of the coexistence region. In contrast with the behavior found for a single-band Hubbard model at half-filling, here, the destruction of metallic quasiparticles leaves behind a preformed gap.

scale of the CT gap instead of U. Second, a $\sim 0.5\%\mathrm{D}T_c$ here is also significantly smaller than the $\sim 3\%$D in the Hubbard model. These quantitative differences all demonstrate that the phase transition is not a one-band type.

In addition to the above difference in the tiny coexistent region, there are more interesting features in the phase diagram in a larger temperature scale. Figure 4 shows the value of the DOS at the chemical potential as a function of the lattice constant and temperature. A significant difference of the above phase diagram compared with the one-band Hubbard model [12,60] is the existence of an insulatorlike phase (in red) even beyond the metallic phase (in light blue) which should end at a_{c1} in the traditional scenario [12,60]. Figure 5 shows the DOS at $a = 2.78$ Å where the system is in a metallic phase at low temperature $T = 12.5$ meV. One can find that, at high temperature $T = 20$ meV, with the destruction of the quasiparticle peak, an insulating gap appears again.

Are these features in the phase diagram the specific results of our hydrogen lattice or the intrinsic properties of

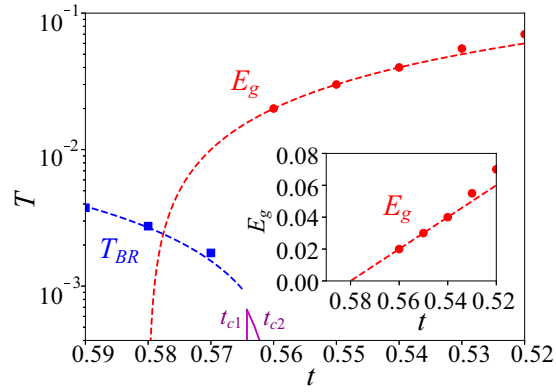

FIG. 6. Phase diagram of a simple two-band model, in the CT regime (see text). The CT gap E_g (here plotted in the same units as temperature) decreases linearly as the bandwidth increases but remains sizeable throughout the coexistence region ($t_c \sim 0.563$), extrapolating to zero further on the metallic side (around $t_g \sim 0.58$). Results shown correspond to $V = 0.217$, and $U = 2$. The results are plotted as a function of t, which sets the bandwidth. Here, we use $\varepsilon_f = 1$ as the unit of energy.

the CT model? To verify this question, we perform the same calculation on a simplified two-band CT model without any long-range screening, which includes one correlated orbital and one higher-energy orbital, given by the Hamiltonian

$$H = \sum_{i\neq j,\sigma}(t-\mu)c^{\dagger}_{i\sigma}c_{j\sigma} + \sum_{i\sigma}(\epsilon_f-\mu)f^{\dagger}_{i\sigma}f_{i\sigma} + \sum_{i,\sigma}(V^{*}_{i\sigma}c^{\dagger}_{i\sigma}f_{i\sigma} + V_{i\sigma}f^{\dagger}_{i\sigma}c_{i\sigma}) + \sum_{i} + U n_{fi\uparrow}n_{fi\downarrow}, \quad \text{(B1)}$$

where $c^{\dagger}_{i\sigma}$, $f^{\dagger}_{i\sigma}$ create one electron at site i with spin σ in two different orbitals, and $n_{fi\sigma} = f^{\dagger}_{i\sigma}f_{i\sigma}$ is the number operator. Only f electrons feel the strong intra-atomic repulsion denoted by U. Here, V is the coupling between two orbitals, and $\epsilon_f > 0$ denotes the CT energy. As the phase diagram shown in Fig. 6, when $U \gg \epsilon_f$, we find a similar strongly suppressed T_c to the hydrogen lattice as well as an insulator phase above the metal phase. The similar phase diagram to that of the hydrogen lattice again implies that the phase transition is less relevant to the long-range screening effect. On the other hand, our results on the simplified CT model indicate these special features in the phase diagram should be the generic behaviors of the CT system instead of the specific results of this particular hydrogen lattice which needs more investigation in the future.

[1] N. F. Mott, Metal-insulator transition, Rev. Mod. Phys. **40**, 677 (1968).

[2] N. Mott, *Metal-Insulator Transitions*, 1st ed. (CRC Press, London, 1990).

[3] M. Imada, A. Fujimori, and Y. Tokura, Metal-insulator transitions, Rev. Mod. Phys. **70**, 1039 (1998).

[4] E. Dagotto, Correlated electrons in high-temperature superconductors, Rev. Mod. Phys. **66**, 763 (1994).

[5] P. A. Lee, N. Nagaosa, and X.-G. Wen, Doping a Mott insulator: Physics of high-temperature superconductivity, Rev. Mod. Phys. **78**, 17 (2006).

[6] J. H. de Boer and E. J. W. Verwey, Semi-conductors with partially and with completely filled $_3d$-lattice bands, Proc. Phys. Soc. **49**, 59 (1937).

[7] W. H. Brito, M. C. O. Aguiar, K. Haule, and G. Kotliar, Metal-insulator transition in VO_2: A DFT + DMFT perspective, Phys. Rev. Lett. **117**, 056402 (2016).

[8] H. Zhang, K. Haule, and D. Vanderbilt, Metal-insulator transition and topological properties of pyrochlore iridates, Phys. Rev. Lett. **118**, 026404 (2017).

[9] A. Damascelli, Z. Hussain, and Z.-X. Shen, Angle-resolved photoemission studies of the cuprate superconductors, Rev. Mod. Phys. **75**, 473 (2003).

[10] P. W. Anderson, Antiferromagnetism. Theory of superexchange interaction, Phys. Rev. **79**, 350 (1950).

[11] N. F. Mott, The basis of the electron theory of metals, with special reference to the transition metals, Proc. Phys. Soc. A **62**, 416 (1949).

[12] A. Georges, G. Kotliar, W. Krauth, and M. J. Rozenberg, Dynamical mean-field theory of strongly correlated fermion systems and the limit of infinite dimensions, Rev. Mod. Phys. **68**, 13 (1996).

[13] G. Kotliar, S. Y. Savrasov, K. Haule, V. S. Oudovenko, O. Parcollet, and C. A. Marianetti, Electronic structure calculations with dynamical mean-field theory, Rev. Mod. Phys. **78**, 865 (2006).

[14] J. Hubbard and B. H. Flowers, Electron correlations in narrow energy bands, Proc. R. Soc. Lond. A **276**, 238 (1963).

[15] J. Hubbard and B. H. Flowers, Electron correlations in narrow energy bands. II. The degenerate band case, Proc. R. Soc. Lond. A **277**, 237 (1964).

[16] J. Hubbard and B. H. Flowers, Electron correlations in narrow energy bands III. An improved solution, Proc. R. Soc. Lond. A **281**, 401 (1964).

[17] M. C. Gutzwiller, Effect of correlation on the ferromagnetism of transition metals, Phys. Rev. Lett. **10**, 159 (1963).

[18] B. J. Powell and R. H. McKenzie, Quantum frustration in organic Mott insulators: From spin liquids to unconventional superconductors, Rep. Prog. Phys. **74**, 056501 (2011).

[19] A. Pustogow, M. Bories, A. Löhle, R. Rösslhuber, E. Zhukova, B. Gorshunov, S. Tomić, J. A. Schlueter, R. Hübner, T. Hiramatsu *et al.*, Quantum spin liquids unveil the genuine Mott state, Nat. Mater. **17**, 773 (2018).

[20] M. J. Rozenberg, G. Moeller, and G. Kotliar, The metal-insulator transition in the Hubbard model at zero temperature II, Mod. Phys. Lett. B **08**, 535 (1994).

[21] K. Haule, C.-H. Yee, and K. Kim, Dynamical mean-field theory within the full-potential methods: Electronic structure of $CeIrIn_5$, $CeCoIn_5$, and $CeRhIn_5$, Phys. Rev. B **81**, 195107 (2010).

[22] K. Haule and T. Birol, Free energy from stationary implementation of the DFT+DMFT functional, Phys. Rev. Lett. **115**, 256402 (2015).

[23] P. Hohenberg and W. Kohn, Inhomogeneous electron gas, Phys. Rev. **136**, B864 (1964).

[24] W. Kohn and L. J. Sham, Self-consistent equations including exchange and correlation effects, Phys. Rev. **140**, A1133 (1965).

[25] W. Metzner and D. Vollhardt, Correlated lattice fermions in $d = \infty$ dimensions, Phys. Rev. Lett. **62**, 324 (1989).

[26] E. Müller-Hartmann, Fermions on a lattice in high dimensions, Int. J. Mod. Phys. B **03**, 2169 (1989).

[27] U. Brandt and C. Mielsch, Thermodynamics and correlation functions of the Falicov-Kimball model in large dimensions, Z. Phys. B **75**, 365 (1989).

[28] V. Janiš, A new construction of thermodynamic mean-field theories of itinerant fermions: Application to the Falicov-Kimball model, Z. Phys. B **83**, 227 (1991).

[29] A. Georges and G. Kotliar, Hubbard model in infinite dimensions, Phys. Rev. B **45**, 6479 (1992).

[30] N. F. Mott, On the transition to metallic conduction in semiconductors, Can. J. Phys. **34**, 1356 (1956).

[31] J. Karp, A. S. Botana, M. R. Norman, H. Park, M. Zingl, and A. Millis, Many-body electronic structure of $NdNiO_2$ and $CaCuO_2$, Phys. Rev. X **10**, 021061 (2020).

[32] K. Pajskr, P. Novák, V. Pokorný, J. Kolorenč, R. Arita, and J. Kuneš, On the possibility of excitonic magnetism in Ir double perovskites, Phys. Rev. B **93**, 035129 (2016).

[33] L. Craco and S. Leoni, LDA + DMFT approach to electronic structure of sodium metal, Phys. Rev. B **100**, 115156 (2019).

[34] R. Xie and H. Zhang, Mixed valence nature of the Ce $4f$ state in $CeCo_5$ based on spin-polarized DFT + DMFT calculations, Phys. Rev. B **106**, 224411 (2022).

[35] I. Leonov, V. I. Anisimov, and D. Vollhardt, Metal-insulator transition and lattice instability of paramagnetic V_2O_3, Phys. Rev. B **91**, 195115 (2015).

[36] We also perform a constrained-RPA calculation implemented by RESPACK [61] and QUANTUM ESPRESSO [62], which gives $U = 12.6$ eV, similar to the bare repulsion.

[37] J. Kondo, Resistance minimum in dilute magnetic alloys, Prog. Theor. Phys. **32**, 37 (1964).

[38] T. K. Ng and P. A. Lee, On-site Coulomb repulsion and resonant tunneling, Phys. Rev. Lett. **61**, 1768 (1988).

[39] P. Blaha, K. Schwarz, F. Tran, R. Laskowski, G. K. H. Madsen, and L. D. Marks, WIEN2K: An APW+lo program for calculating the properties of solids, J. Chem. Phys. **152**, 074101 (2020).

[40] D. Jérome, T. M. Rice, and W. Kohn, Excitonic insulator, Phys. Rev. **158**, 462 (1967).

[41] W. Kohn, Excitonic phases, Phys. Rev. Lett. **19**, 439 (1967).

[42] S. Biermann, F. Aryasetiawan, and A. Georges, First-principles approach to the electronic structure of strongly correlated systems: Combining the *GW* approximation and dynamical mean-field theory, Phys. Rev. Lett. **90**, 086402 (2003).

[43] T. Ayral, S. Biermann, and P. Werner, Screening and nonlocal correlations in the extended Hubbard model from self-consistent combined *GW* and dynamical mean field theory, Phys. Rev. B **87**, 125149 (2013).

[44] P. Hansmann, T. Ayral, L. Vaugier, P. Werner, and S. Biermann, Long-range Coulomb interactions in surface systems: A first-principles description within self-consistently combined *GW* and dynamical mean-field theory, Phys. Rev. Lett. **110**, 166401 (2013).

[45] F. Petocchi, F. Nilsson, F. Aryasetiawan, and P. Werner, Screening from e_g states and antiferromagnetic correlations in $d^{(1,2,3)}$ perovskites: A *GW* + EDMFT investigation, Phys. Rev. Res. **2**, 013191 (2020).

[46] R. Chitra and G. Kotliar, Effect of long range Coulomb interactions on the Mott transition, Phys. Rev. Lett. **84**, 3678 (2000).

[47] A. Rubtsov, M. Katsnelson, and A. Lichtenstein, Dual boson approach to collective excitations in correlated fermionic systems, Ann. Phys. **327**, 1320 (2012).

[48] L. Huang, T. Ayral, S. Biermann, and P. Werner, Extended dynamical mean-field study of the Hubbard model with long-range interactions, Phys. Rev. B **90**, 195114 (2014).

[49] E. G. C. P. van Loon, H. Hafermann, A. I. Lichtenstein, A. N. Rubtsov, and M. I. Katsnelson, Plasmons in strongly correlated systems: Spectral weight transfer and renormalized dispersion, Phys. Rev. Lett. **113**, 246407 (2014).

[50] H. Hafermann, E. G. C. P. van Loon, M. I. Katsnelson, A. I. Lichtenstein, and O. Parcollet, Collective charge excitations of strongly correlated electrons, vertex corrections, and gauge invariance, Phys. Rev. B **90**, 235105 (2014).

[51] G. Rohringer, H. Hafermann, A. Toschi, A. A. Katanin, A. E. Antipov, M. I. Katsnelson, A. I. Lichtenstein, A. N. Rubtsov, and K. Held, Diagrammatic routes to nonlocal correlations beyond dynamical mean field theory, Rev. Mod. Phys. **90**, 025003 (2018).

[52] M. Schüler, E. G. C. P. van Loon, M. I. Katsnelson, and T. O. Wehling, Thermodynamics of the metal-insulator transition in the extended Hubbard model, SciPost Phys. **6**, 067 (2019).

[53] H. Terletska, S. Iskakov, T. Maier, and E. Gull, Dynamical cluster approximation study of electron localization in the extended Hubbard model, Phys. Rev. B **104**, 085129 (2021).

[54] D. Vollhardt, K. Byczuk, and M. Kollar, Dynamical mean-field theory, in *Strongly Correlated Systems: Theoretical Methods*, edited by A. Avella and F. Mancini (Springer, Berlin, 2012), pp. 203–236.

[55] A. Georges and W. Krauth, Physical properties of the half-filled Hubbard model in infinite dimensions, Phys. Rev. B **48**, 7167 (1993).

[56] M. J. Rozenberg, G. Kotliar, and X. Y. Zhang, Mott-Hubbard transition in infinite dimensions. II, Phys. Rev. B **49**, 10181 (1994).

[57] S. R. Schofield, P. Studer, C. F. Hirjibehedin, N. J. Curson, G. Aeppli, and D. R. Bowler, Quantum engineering at the silicon surface using dangling bonds, Nat. Commun. **4**, 1649 EP (2013).

[58] M. Jarrell and J. Gubernatis, Bayesian inference and the analytic continuation of imaginary-time quantum Monte Carlo data, Phys. Rep. **269**, 133 (1996).

[59] W. F. Brinkman and T. M. Rice, Application of Gutzwiller's variational method to the metal-insulator transition, Phys. Rev. B **2**, 4302 (1970).

[60] H. Eisenlohr, S.-S. B. Lee, and M. Vojta, Mott quantum criticality in the one-band Hubbard model: Dynamical mean-field theory, power-law spectra, and scaling, Phys. Rev. B **100**, 155152 (2019).

[61] K. Nakamura, Y. Yoshimoto, Y. Nomura, T. Tadano, M. Kawamura, T. Kosugi, K. Yoshimi, T. Misawa, and Y. Motoyama, RESPACK: An *ab initio* tool for derivation of effective low-energy model of material, Comput. Phys. Commun. **261**, 107781 (2021).

[62] P. Giannozzi, O. Baseggio, P. Bonfà, D. Brunato, R. Car, I. Carnimeo, C. Cavazzoni, S. de Gironcoli, P. Delugas, F. Ferrari Ruffino *et al.*, QUANTUM ESPRESSO toward the exascale, J. Chem. Phys. **152**, 154105 (2020).